Accepted Manuscript

Physical Properties and Long-Term Evolution of the Debris Clouds Produced by Two Catastrophic Collisions in Earth Orbit

C. Pardini, L. Anselmo

PII: S0273-1177(11)00243-2
DOI: 10.1016/j.asr.2011.04.006
Reference: JASR 10552

To appear in: *Advances in Space Research*

Received Date: 19 October 2010
Accepted Date: 8 April 2011

Physical Properties and Long-Term Evolution of the Debris Clouds Produced by Two Catastrophic Collisions in Earth Orbit

C. Pardini[a] and L. Anselmo[b]

[a, b]*Space Flight Dynamics Laboratory, ISTI/CNR, Via G. Moruzzi 1, 56124 Pisa, Italy*

[a]*E-mail: Carmen.Pardini@isti.cnr.it*
[b]*E-mail: Luciano.Anselmo@isti.cnr.it*

Abstract

The population of cataloged orbital debris increased by approximately 40% in just a couple of years, from January 2007 to February 2009. This was due to two collisions in space, which involved the catastrophic destruction of three intact satellites (Fengyun 1C, Cosmos 2251 and Iridium 33) in high inclination orbits. Both events occurred in the altitude range already most affected by previous launch activity and breakup events, thus boosting the cataloged population in low Earth orbit by more than 60%.

In order to investigate the long-term orbit evolution of the three resulting debris clouds and to assess their lifetimes, an updated and more refined estimate of the ballistic parameter and area-to-mass ratio distributions of the fragments was accomplished. On 20 April 2010, the fraction of cataloged objects in orbit with a high area-to-mass ratio (≥ 1 m^2/kg) was approximately 3% for the Fengyun 1C cloud, 2% for the Cosmos 2251 cloud, and 18% for the Iridium 33 cloud. This was less than had been obtained previously, due to the greater decay rate of these objects. Their relative depletion will continue in the coming years and most will have reentered the atmosphere by 2015.

The Iridium 33 cloud will be the fastest to decay from orbit, with 50% of the cataloged fragments left in space around 2015, and 10% around 2024. The Cosmos 2251 cloud will stay a little while longer, with 50% of the cataloged fragments left in space around 2021, and 10% around 2037. The Fengyun 1C cloud, on the other hand, will burden the environment significantly longer, with 50% of the cataloged fragments still in orbit around 2025 and 10% left in space around 2090.

1. Introduction

After two decades of slightly declining growth rate, thanks also to the advancing implementation of mitigation measures adopted worldwide, the population of cataloged orbital debris around the Earth increased by approximately 40% in just a couple of years, from January 2007 to February 2009. This sudden increase was caused by two collisions in space involving the catastrophic destruction of three intact satellites (Fengyun 1C, Cosmos 2251 and Iridium 33) in high inclination orbits (Anonymous, 2010a). Both events occurred in the altitude range already most affected by previous launches and breakup events (Figure 1), thus boosting the cataloged population in Low Earth Orbit (LEO), i.e. below the altitude of 2000 km, by more than 60% (Anonymous, 2010b). To give a rough idea of the impact of such occurrences on the circumterrestrial environment, it is sufficient to realize that, in numerical terms, they increased the number of cataloged objects around the Earth and in LEO by the same amount produced, respectively, in the 22 and 36 years of space activity preceding the Fengyun 1C intentional breakup.

This occurred on 11 January 2007, around 22:25:40 UTC, when the 880 kg defunct weather spacecraft (International Designator: 1999-025A; US Catalog Number: 25730), launched on 10 May 1999 into a sun-synchronous orbit with a CZ-4B booster from the Taiyuan Satellite Launch Center, was destroyed over central China as a result of the first successful Chinese anti-satellite

(ASAT) weapon test. It was carried out using a direct ascent interception with a sub-orbital kinetic energy kill vehicle launched by an SC-19 missile, which was fired from a mobile ground platform close to the Xichang Satellite Launch Center (Pardini and Anselmo, 2007).

Before the collision, the orbit of Fengyun 1C presented a minimum geodetic altitude of 855 km, a maximum geodetic altitude of 876 km and an inclination of 98.6°. The impact occurred at a geodetic altitude of approximately 863 km over central China, with a relative velocity of 9.4 km/s (Pardini and Anselmo, 2007; 2009), spreading the resulting fragments throughout LEO and beyond, between 200 and 4000 km (Figure 2). As of 1 October 2010, the US Space Surveillance Network (SSN) had cataloged 3037 objects larger than 4-5 cm, of which only 95 (≅ 3.1%) had reentered. However, more than 300 additional fragments were being tracked, waiting for official cataloging (Anonymous, 2010b), and over 150,000 fragments larger than 1 cm had also probably been generated (Matney et al., 2008; Anonymous, 2009).

On 10 February 2009, at around 16:56:00 UTC, two satellites collided at a geodetic altitude of approximately 789 km above Siberia, with a relative impact velocity of 11.6 km/s, disseminating the resulting fragments throughout LEO, between 200 and 1800 km (Anselmo and Pardini, 2009b; Figure 3). Although in the past at least three unintentional hypervelocity impacts between cataloged objects had been documented in space, this was the first accidental catastrophic collision between two intact satellites. Cosmos 2251 (International Designator: 1993-036A; US Catalog Number: 22675) was a 900 kg Strela-2 Russian spacecraft used for military communications, which had been decommissioned more than ten years earlier. Before the collision, its orbit exhibited a minimum geodetic altitude of 784 km, a maximum geodetic altitude of 826 km, and an inclination of 74.0°. Instead Iridium 33 (International Designator: 1997-051C; US Catalog Number: 24946) was an operational 556 kg spacecraft of the homonymous private constellation for worldwide voice and data communications using handheld satellite phones. Before the accidental crash, its orbit presented a minimum geodetic altitude of 779 km, a maximum geodetic altitude of 808 km, and an inclination of 86.4°.

Based on the last Two-Line Elements (TLE) sets released by the US Joint Space Operations Center (JSpOC), the predicted miss distance at the time the collision took place would have been 698 m, making the chance of a crash extremely remote (Anselmo, 2009). However, the last TLEs were 22 hours old for Iridium 33, and 29 hours old for Cosmos 2251, which coupled with the TLE intrinsic uncertainty, made such a miss distance estimate quite inaccurate. Nevertheless, even a post-event analysis using SSN observations obtained closer to the event, gave a miss distance of 223 m and a negligible collision probability (Newman et al, 2009). It was later learned that the Iridium 33 satellite had performed two small maneuvers several hours before the crash, as part of its routine constellation maintenance. By including the planned maneuvers in the post-event analysis, the estimated miss distance decreased to 60 m, with a corresponding impact probability of about 5×10^{-3} (Newman et al, 2009). Therefore, Iridium 33 was basically maneuvered into the abandoned Cosmos 2251, because the operator of the Iridium constellation lacked relevant and accurate information concerning the whereabouts of the Cosmos satellite.

As of 1 October 2010, the SSN had cataloged 1347 Cosmos 2251 fragments larger than 4-5 cm, of which 61 (≅ 4.5%) had reentered. In addition, approximately 200 other objects were being tracked and were awaiting formal cataloging. The creation of about 40,000 fragments larger than 1 cm was also inferred by a dedicated NASA measurement campaign using Goldstone and Haystack radar observations (Matney, 2010). At the same epoch, 528 Iridium 33 fragments larger than 4-5 cm, of which 30 (≅ 5.7%) had reentered, were officially cataloged. In addition, about 100 further objects were being tracked and were awaiting official cataloging. Moreover, the creation of about 30,000 fragments larger than 1 cm was deduced by a dedicated NASA measurement campaign using Haystack radar observations (Matney, 2010).

Following the breakups, all the fragments were almost in the same orbital plane as the respective parent satellite. However, due to the differential precession of the nodes induced by the perturbations, the near sun-synchronous orbits of the Fengyun 1C debris had completely enveloped the Earth within about 7-8 months. More than three years after the spacecraft destruction, it had formed a roughly uniform shell, excluding the polar regions (Figures 4 and 5). The argument of perigee distribution was also relatively even (Figure 6).

On the other hand, more than one year after the satellite crash, owing to the smaller spread in the semi-major axis of the fragments (Figure 3), the Cosmos 2251 debris was still not evenly distributed around the Earth (Figures 4 and 5), and needed a few additional years to do so (Pardini and Anselmo, 2010). Even the distribution of the argument of perigee was still far from uniform (Figure 6). Regarding Iridium 33, the even smaller semi-major axis spread of the fragments (Figure 3), coupled with the nearly polar initial inclination, resulted in a still narrower nodal dispersion of debris orbits, more than one year after the breakup (Figures 4 and 5). Due to the slowness of the process and the concomitant orbital decay of the cloud, a modest node dispersion will persist for many years and most of the fragments will reenter the atmosphere before the creation of a roughly uniform debris shell around the Earth (Pardini and Anselmo, 2010). The argument of perigee, however, was already quite well scattered more than 14 months after the accidental impact, although not yet evenly distributed (Figure 6).

Both collisions, which were by far the worst breakups recorded in more than half century of orbital space activity (Anonymous, 2010c), occurred in the altitude range already most populated by artificial debris (Figure 1). At around the original height of Fengyun 1C, the cataloged object density increased by more than 150%, while at around the height of the collision between Cosmos 2251 and Iridium 33, the cataloged object density increased by more than 120%. However, the environmental impact was significant in the overall altitude range of between 600 and 1000 km, where the debris density due to past space activities was already high.

In order to investigate the lifetime of the fragments and the long-term significance of these major collisional breakups, the physical characteristics of the new debris clouds, in terms of ballistic parameter and area-to-mass ratio (*A/M*) distributions, were preliminarily derived from a decay analysis of representative samples of cataloged objects, as reported in Pardini and Anselmo (2009) for Fengyun 1C, and in Anselmo and Pardini (2009b) for Cosmos 2251 and Iridium 33. The analysis described in this paper represents a substantial refinement and update of those preliminary investigations, with improved physical parameter estimations and lifetime predictions for the three debris clouds.

2. Estimation of the physical properties of the debris clouds

In order to assess the evolution of the debris clouds, knowledge of the ballistic parameter and orbit of each fragment was needed. In theory, for cataloged objects, this information is coded in the TLEs distributed through the Space Track organization (www.space-track.org). The ballistic parameter B, defined as the product between the drag coefficient C_D and the object area-to-mass ratio A/M, i.e. $B = C_D\, A/M$, could have been obtained from the so-called "BSTAR" (B^*) value given in each TLE (Hoots and Roehrich, 1980; Hoots et al., 2004; Vallado et al., 2006). In fact, according to the TLE orbital theory, the ballistic parameter B can be computed from B^* in the following way (Vallado, 2001):

$$B = 12.741621 B^* \text{ m}^2/\text{kg}. \tag{1}$$

However, the underlying TLE orbital theory assumes an atmospheric model that does not vary with solar activity, i.e. it considers a fixed density at any given height. The observed orbital decay is fitted with an appropriate value of the B^* parameter. Therefore, during periods of low solar activity, and correspondingly lower than average atmospheric densities at the altitudes of interest, such as during the deep solar minimum between the end of cycle 23 and the beginning of cycle 24, in 2007-2010 (Emmert et al., 2010; see Figure 7), the values of B^* are smaller than average and the corresponding ballistic parameters obtained from Eq. (1) are systematically underestimated, even by a large amount. In addition, the B^* values estimated for each individual fragment displayed very wide variations from one TLE to another. To give an idea of the variability observed, it is sufficient to say that for a typical Fengyun 1C debris, for which in many cases several hundred TLEs were available, the B^* standard deviation was generally several tens percent of the mean value, irrespective of the initial perigee altitude. The same was also basically true for the typical debris of Cosmos 2251 and Iridium 33.

Of course, good values of B might have been determined by fitting the observed orbital decay of each fragment, over relatively long time spans, using accurate orbit propagators and atmospheric density models (Pardini and Anselmo, 2008). However, due to the huge number of fragments generated, this would have required the allocation of an excessive amount of dedicated resources. Therefore, an alternative hybrid approach, which was both accurate and practicable, was devised and applied to the Fengyun 1C, Cosmos 2251 and Iridium 33 debris (Pardini and Anselmo, 2008c; 2009; Anselmo and Pardini, 2009b). In this paper the analysis was substantially reviewed, refined and updated, by taking into account the few reentries and the several hundred new objects that have since been cataloged.

First of all, for each debris cloud, the cataloged fragments were grouped into different sets, depending on their perigee altitude (P_H). In fact, air drag, on which the B fitting was inherently based, is mostly active around the perigee height of elliptical orbits (King-Hele, 1987), and for nearly circular orbits, of course, the perigee height is close to the average height. Then, a random subset of cataloged objects, corresponding to 10% of the total, was taken from every perigee altitude set, and the orbital decay of each of the sampled fragments was analyzed over appreciably long intervals of time. The corresponding ballistic parameters were therefore determined by fitting, in a least squares sense, the semi-major axis decay inferred from the historical TLEs of every sampled debris.

The semi-major axis decay fits were carried out with a special perturbation numerical code (CDFIT), using the same force model implemented in the SATRAP orbit propagator (Pardini and Anselmo, 1994). All the relevant orbit perturbations were considered, namely geopotential harmonics up to the 8th degree and order (EGM96 model, Lemoine et al., 1998), third body attraction of the Moon and the Sun, direct solar radiation pressure with eclipses, assuming a radiation pressure coefficient equal to 1.2, and aerodynamic drag. The Jacchia-Roberts 1971 model, as implemented in Cappellari et al. (1976), was used to describe the atmospheric density.

The following step consisted in obtaining the scaling factor, defined as the ratio between the fitted value of the ballistic parameter and the value obtained by applying Eq. (1) to B^*, for each sampled object of every perigee altitude set. In order to do this, the fitted ballistic parameter was compared with the value of B obtained by applying Eq. (1) to the average B^*, i.e. the arithmetic mean of the values of B^* determined by the SSN over the same time interval used for the fit.

At this point, a mean scaling factor and its standard deviation were computed for each sampled perigee altitude subset. Then, assuming a Gaussian distribution, using the mean and standard deviation thus found, randomly generated scaling factors were applied to the values of B obtained by applying Eq. (1) to all the remaining fragments of each perigee altitude set. Finally, by merging the perigee altitude sets of the fragments corresponding to the same parent satellite, the rescaled ballistic parameter distributions of the three whole debris clouds were obtained.

3. Ballistic parameter distributions of the three debris clouds

Figure 8 and Table 1 show the perigee altitude distribution of the three debris clouds at the reference epoch of the analysis, i.e. 20 April 2010. In order to apply the procedure outlined in the previous section, the cataloged objects of each cloud were partitioned into two or three perigee altitude sets, depending on the debris height distribution and number (Figure 8 and Table 1). Then, from each set, approximately 10% of the objects were randomly sorted. For Fengyun 1C, the three samples consisted of 52 objects with $P_H < 600$ km, 114 with 600 km $\leq P_H \leq$ 800 km and 110 with $P_H > 800$ km, i.e. 276 objects in total. For Cosmos 2251, the three samples consisted of 19 objects with $P_H < 500$ km, 48 with 500 km $\leq P_H \leq$ 700 km and 57 with $P_H > 700$ km, i.e. 124 objects in total. Finally, for Iridium 33, the two samples consisted of 27 objects with $P_H < 750$ km and 31 with $P_H \geq 750$ km, i.e. 58 objects in total.

The observed semi-major axis decay of all the objects in each sample was therefore fitted, typically using the historical TLEs available during the 12-14 months preceding the reference epoch of the analysis. On the basis of the fitted ballistic parameters thus determined, it was therefore possible to infer the statistical distribution of the scaling factors, corresponding to the values of B obtained by applying Eq. (1). Table 2 summarizes the new results obtained for the scaling factors, while the overall distribution of the ballistic parameters inferred from the orbital decay analysis is presented in Figure 9 for Fengyun 1C, in Figure 10 for Cosmos 2251, and in Figure 11 for Iridium 33.

Figure 12 presents the related *A/M* distributions found for the three debris clouds, assuming $C_D = 2.2$, i.e. the "classical" standard value adopted early in the space age and, in particular, by Jacchia to develop his thermospheric density models based on satellite decay analysis (King-Hele, 1987; Moe and Moe, 2005). For the Fengyun 1C cloud, the new results were in good agreement with the previous estimates, based on less cataloged debris and smaller statistical samples (Pardini and Anselmo, 2008c; 2009; Anselmo and Pardini, 2010). The qualitative agreement was also satisfactory with the results presented by Liou and Johnson (2008) and Stansbery et al. (2008). Even for the Cosmos 2251 and the Iridium 33 clouds, the new results were in good agreement with the previous estimates, again based on less cataloged debris and smaller statistical samples (Anselmo and Pardini, 2009b; 2010). Wang (2010) obtained similar distributions, with basically the same extrema, but with barycenters somewhat shifted towards lower area-to-mass ratios.

One change observed with respect to the previous results was the relative reduction in cataloged fragments with high *A/M* (≥ 1 m^2/kg) still in orbit. In fact, based on the earlier analyses, they amounted to about 5% of the total for Fengyun 1C, again about 5% for Cosmos 2251, and almost 26% for Iridium 33 (Anselmo and Pardini, 2009b; 2010). As expected, due to the greater decay rate of high *A/M* objects and the continuing addition to the catalog of objects characterized by typically smaller area-to-mass ratios, the new distributions presented a relative loss of fragments with $A/M \geq 1$ m^2/kg (Pardini and Anselmo, 2010). At the reference epoch of the new analysis, i.e. 20 April 2010, it was found that the high *A/M* objects still in orbit amounted to about 3% of the total for Fengyun 1C, about 2% for Cosmos 2251, and approximately 18% for Iridium 33.

The presence of a non negligible number of fragments with 1 m^2/kg $< A/M <$ 100 m^2/kg, that is with area-to-mass ratios similar to those of a debris population discovered a few years ago in geosynchronous orbits (Schildknecht et al., 2004, 2008; Agapov et al., 2005), shows that the generation of trackable orbital debris with average *A/M* hundreds or thousands of times greater than those of intact satellites might be more common than previously supposed. Such objects are a likely consequence of fragmentation events, involving for instance spacecraft and rocket bodies with multi-layered insulation (MLI) blankets and other low density composite materials (Liou and Weaver, 2004). This might explain why the *A/M* distribution of the Iridium 33 cloud was systematically shifted towards higher values: the Iridium satellites make considerable use of low density materials, much more, in fact, than traditional Chinese or Russian spacecraft, such as Fengyun 1C or Cosmos 2251.

4. Long-term evolution of the debris clouds

Having determined rescaled ballistic parameters for all the cataloged fragments in orbit, as of 20 April 2010, all the objects of the three debris clouds were individually propagated with the

SATRAP special perturbation numerical code (Pardini and Anselmo, 1994). This was done taking into account the most important perturbations, namely the EGM96 Earth's gravity field harmonics, up to the 5th order and degree, air drag, luni-solar third body attraction and solar radiation pressure with eclipses, assuming a radiation pressure coefficient equal to 1.2. To estimate the effects of air drag, the Jacchia-Roberts 1971 density model was adopted, together with the European Space Agency (ESA) long-term predictions of the geomagnetic planetary index A_P, issued on 3 April 2010 on the Inter-Agency Space Debris Coordination Committee (IADC) Common Database (mas15.esoc.esa.de:8000), and with the National Aeronautics and Space Administration (NASA) long-term predictions of the 10.7 cm solar flux proxy, issued on 1 March 2010 and recommended for use with the last version of NASA's Debris Assessment Software (orbitaldebris.jsc.nasa.gov/mitigate/das.html).

Figures 13, 14 and 15 show how the *A/M* distribution of the cataloged debris left in orbit will change over the next 30 years, due to atmospheric reentry, for the Fengyun 1C, Cosmos 2251 and Iridium 33 clouds, respectively. The progressive expected depletion of higher *A/M* fragments is evident and most, if not all, of the objects with $A/M \geq 1$ m^2/kg will be removed from space by 2015. This is in agreement with the hypothesis that the production of debris with very high area-to-mass ratios might be quite common as a consequence of on-orbit breakups. However, it also highlights that a substantial population of such objects may accumulate and be discovered only rather above LEO, due to a significantly longer orbital lifetime (Pardini and Anselmo, 2008b; Valk et al., 2008; Anselmo and Pardini, 2009a; 2010).

Figure 16 summarizes the expected burden of the three debris clouds on the circumterrestrial environment over the next 100 years, in terms of the percentage of cataloged fragments left in orbit, as of 20 April 2010. Of course, these predictions are only indicative, due to the considerable uncertainties affecting solar activity forecasts, even over much shorter intervals of time.

In any case, the results obtained confirmed the faster decay predicted for the Iridium 33 debris cloud, with 50% of the cataloged fragments reentering the atmosphere by around 2015, 90% by around 2024, and less than 1% left in orbit around 2050-2060. Concerning the Cosmos 2251 debris cloud, the corresponding figures were 50% of the cataloged fragments reentering the atmosphere by around 2021, 90% by around 2037, and less than 1% left in orbit around 2090. Various previous estimates obtained roughly comparable results up to 2020 (Johnson, 2009; Anselmo and Pardini, 2009b; Wang, 2010), but the quantitative discrepancies could become quite significant at later epochs. However, there was broad agreement on the fact that the Iridium 33 cloud will decay much faster than the cloud resulting from the Cosmos 2251 breakup, and that the overall number of cataloged debris in orbit from the accidental collision will drop to less than 10% of its initial value by 2070-2080.

Unfortunately, even according to these latest results, the Fengyun 1C debris cloud will affect the environment significantly longer than the other two clouds (Figure 16), with 50% of the cataloged fragments still in orbit around 2025 and 10% still in orbit around 2090. These new projections were in very good agreement with previous estimations (Liou and Johnson, 2008; Johnson et al., 2008; Pardini and Anselmo, 2008c; 2009), and nearly 8% of the fragments, corresponding to about 240 cataloged objects, might be found in orbit more than one century after the ASAT test.

5. Conclusions

Following two catastrophic collisions in space, involving the complete destruction of three intact satellites (Fengyun 1C, Cosmos 2251 and Iridium 33) in high inclination orbits, an updated and more refined estimate of the ballistic parameter and area-to-mass ratio distributions of the three resulting debris clouds was completed.

Both events occurred in the altitude range already most affected by previous launch activity and breakup events, leading to the progressive formation of new shells of debris around the Earth, at least in the cases of the objects generated by Fengyun 1C and Cosmos 2251. However, due to the nearly polar inclination and the relatively limited spread in semi-major axis, the orbit planes of most of the Iridium 33 fragments will continue to present a modest ascending node dispersion for several years to come. In any case, the two breakup events increased the collision probability by a factor of two with cataloged debris at the operational altitude of the Iridium constellation.

Considering the cataloged fragments still in orbit on 20 April 2010, the fraction of those with a high area-to-mass ratio ($\geq 1\ m^2/kg$) was about 3% for the Fengyun 1C cloud, 2% for the Cosmos 2251 cloud, and 18% for the Iridium 33 cloud. This was less than obtained in previous analyses, but was not surprising due to the greater decay rate of high area-to-mass ratio objects. This relative depletion of high *A/M* debris will continue in the future and most of the objects with $A/M \geq 1\ m^2/kg$ will have reentered the atmosphere by 2015.

The Iridium 33 cloud will be the fastest to decay from orbit, with 50% of the cataloged fragments left in space around 2015, 10% remaining around 2024, and less than 1% still around after the mid-century. The Cosmos 2251 cloud will remain in space a little while longer, with 50% of the cataloged fragments left in space around 2021, 10% remaining around 2037, and less than 1% left in orbit around 2090. The Fengyun 1C cloud, on the other hand, will affect the environment for significantly longer, with 50% of the cataloged fragments still in orbit around 2025 and 10% left in space around 2090.

In conclusion, the catastrophic collisional fragmentation of three intact satellites, which has led to the formation of the three worst debris clouds ever in a region of space that was already densely populated by orbital debris, represented a severe blow to the international mitigation efforts that had been carried out during the previous 20-30 years. Fortunately for the circumterrestrial environment, the debris clouds generated by the accidental collision between Cosmos 2251 and Iridium 33 will decay quite rapidly, with a total of about 150 cataloged debris left in orbit after 30 years. However, the consequences of the ASAT test which destroyed Fengyun 1C will be felt for much longer, with almost 250 cataloged debris still in orbit after one century.

Acknowledgments

The results described in this paper were presented at the 38th COSPAR Scientific Assembly, held in Bremen, Germany, on 18-25 July 2010.

We would like to thank the US Space Surveillance Network, for making available the two-line elements of the Fengyun 1C, Cosmos 2251 and Iridium 33 fragments.

References

Agapov, V., Biryukov, V., Kiladze, R., Molotov, I., Rumyantsev, V., Sochilina, A., Titenko, V. Faint GEO objects search and orbital analysis, in: Danesy, D. (Ed.), Proceedings of the Fourth European Conference on Space Debris, ESA SP-587, ESA Publications Division, Noordwijk, The Netherlands, pp. 119–124, 2005.

Anonymous. Fengyun-1C debris: Two years later. Orbital Debris Quarterly News, Vol. 13, Issue 1, p. 2, January 2009.

Anonymous. Monthly number of objects in Earth orbit by object type. Orbital Debris Quarterly News, Vol. 14, Issue 1, p. 12, January 2010a.

Anonymous. Update on three major debris clouds. Orbital Debris Quarterly News, Vol. 14, Issue 2, p. 4, April 2010b.

Anonymous. Top ten satellite breakups. Orbital Debris Quarterly News, Vol. 14, Issue 3, pp. 2-3, April 2010c.

Anselmo, L. ASI report on debris mitigation at the 27th IADC. Presentation at Working Group 4. Proceedings of the 27th Inter-Agency Space Debris Coordination Committee Meeting, CD-ROM, ESA/ESOC, Darmstadt, Germany, 25-27 March 2009.

Anselmo, L., Pardini, C. Dynamical evolution of high area-to-mass ratio debris released into GPS orbits. Advances in Space Research 43 (10), 1491-1508, 2009a.

Anselmo, L., Pardini, C. Analysis of the consequences in low Earth orbit of the collision between Cosmos 2251 and Iridium 33. Proceedings of the 21st International Symposium on Space Flight Dynamics, CD-ROM, ACM 2009-294, CNES, Toulouse, France, November 2009b.

Anselmo, L., Pardini, C. Long-term dynamical evolution of high area-to-mass ratio debris released into high Earth orbits. Acta Astronautica 67 (1-2), 204-216, 2010.

Cappellari, J.O., Velez, C.E., Fuchs, A.J. (Eds.). Mathematical theory of the Goddard Trajectory Determination System. NASA/GSFC Report, GSFC X-582-76-77, Greenbelt, MD, USA, 1976.

Emmert, J.T., Lean, J.L., Picone, J.M. Record-low thermospheric density during the 2008 solar minimum. Geophysical Research Letters, 37, L12102, 2010.

Hoots, F.R., Roehrich, R.L. Models for propagation of NORAD elements sets. Spacetrack Report No. 3, Project Spacetrack, Aerospace Defense Command, United States Air Force, Colorado Springs, CO, USA, December 1980.

Hoots, F.R., Schumacher, P.W., Glover, R.A. History of analytical orbit modeling in the U.S. space surveillance system. Journal of Guidance, Control, and Dynamics 27 (2), 174-185, 2004.

Johnson, N.L. Consequences of the collision of Iridium 33 and Cosmos 2251. NASA presentation at the 52nd Session of the Committee on the Peaceful Uses of Outer Space (COPUOS), United Nations, Vienna, Austria, 3-12 June 2009.

Johnson, N.L., Stansbery, E., Liou, J.-C., Horstman, M., Stokely, C., Whitlock, D. The characteristics and consequences of the break-up of the Fengyun-1C spacecraft. Acta Astronautica 63, 128-135, 2008.

King-Hele, D. Satellite Orbits in an Atmosphere, Theory and Applications. Blackie, Glasgow and London, United Kingdom, 1987.

Lemoine, F.G., Kenyon, S.C., Factor, J.K., et al. The development of the joint NASA GSFC and NIMA geopotential model EGM96, NASA/TP-1998-206861. NASA Goddard Space Flight Center, Greenbelt, MD, USA, July 1998.

Liou, J.-C., Johnson, N.L. Characterization of the cataloged Fengyun-1C fragments and their long-term effect on the LEO environment. Presented at the 37th COSPAR Scientific Assembly, Montréal, Canada, PEDAS1-0013-08, 13-20 July 2008.

Liou, J.-C., Weaver, J.K. Orbital evolution of GEO debris with very high area-to-mass ratios. Orbital Debris Quarterly News 8 (3), 6-7, 2004.

Matney, M. Small debris observations from the Iridium 33/Cosmos 2251 collision. Orbital Debris Quarterly News, Vol. 14, Issue 2, pp. 6-8, April 2010.

Matney, M., Stansbery, E., Liou, J.-C., Stokely, C., Horstman, M., Whitlock, D. Measurements of the small particle debris cloud from the 11 January 2007 Chinese anti-satellite test. Proceedings of the 59th International Astronautical Congress, DVD, Glasgow, Scotland, United Kingdom, Paper IAC-08-A6.1.08, September 2008.

Moe, K., Moe, M.M. Gas-surface interactions and satellite drag coefficients. Planetary and Space Science 53, 793-801, 2005.

Newman, L.K., Frigm, R., McKinley, D. It's not a big sky after all: Justification for a close approach prediction and risk assessment process. Paper AAS 09-369, presented at the 2009 AAS/AIAA Astrodynamics Specialist Conference, Pittsburgh, PA, USA, 9-13 August 2009.

Pardini, C., Anselmo, L. SATRAP: Satellite reentry analysis program. Internal Report C94-17, CNUCE Institute, Consiglio Nazionale delle Ricerche (CNR), Pisa, Italy, 30 August 1994.

Pardini, C., Anselmo, L. Evolution of the debris cloud generated by the Fengyun-1C fragmentation event. Proceedings of the 20th International Symposium on Space Flight Dynamics, CD-ROM, NASA CP-2007-214158, Goddard Space Flight Center, Greenbelt, Maryland, USA, September 2007.

Pardini, C., Anselmo, L. Impact of the time span selected to calibrate the ballistic parameter on spacecraft re-entry predictions. Advances in Space Research 41 (7), 1100-1114, 2008a.

Pardini, C., Anselmo, L. Long-term evolution of geosynchronous orbital debris with high area-to-mass ratios. Transactions of The Japan Society for Aeronautical and Space Sciences 51 (171), 22-27, 2008b.

Pardini, C., Anselmo, L. Assessment of the consequences of the Fengyun-1C breakup in low Earth orbit. Presented at the 37th COSPAR Scientific Assembly, Montréal, Canada, PEDAS1-0012-08, 13-20 July, 2008c.

Pardini, C., Anselmo, L. Assessment of the consequences of the Fengyun-1C breakup in low Earth orbit. Advances in Space Research 44 (5), 545-557, 2009.

Pardini, C., Anselmo, L. Physical properties and long-term evolution of the debris clouds produced by two catastrophic collisions in Earth orbit. Presented at the 38th COSPAR Scientific Assembly, Bremen, Germany, PEDAS1-0015-10, 18-25 July 2010.

Schildknecht, T., Musci, R., Ploner, M., Beutler, G., Flury, W., Kuusela, J., de Leon Cruz, J., de Fatima Dominguez Palmero, L. Optical observations of space debris in GEO and in highly-eccentric orbits. Advances in Space Research 34, 901-911, 2004.

Schildknecht, T., Musci, R., Flohrer, T. Properties of the high area-to-mass ratio space debris population at high altitudes. Advances in Space Research 41, 1039-1045, 2008.

Stansbery, G., Matney, M., Liou, J.-C., Whitlock, D. A comparison of three catastrophic on-orbit collisions. Proceedings of the 59th International Astronautical Congress, DVD, Glasgow, Scotland, United Kingdom, Paper IAC-08-A6.1.07, September 2008.

Valk, S., Lemaître, A., Anselmo L. Analytical and numerical investigations of geosynchronous space debris with high area-to-mass ratios influenced by solar radiation pressure, Advances in Space Research 41 (7), 1077-1090, 2008.

Vallado, D.A. Fundamentals of Astrodynamics and Applications, second ed. Microcosm Press and Kluwer Academy Publishers, Dordrecht, The Netherlands, p. 114, 2001.

Vallado, D.A., Crawford, P., Hujsak, R., Kelso, T.S. Revisiting spacetrack report #3. Paper AIAA 2006-6753, presented at the AIAA/AAS Astrodynamics Specialist Conference, Keystone, CO, 21-24 August 2006.

Wang, T. Analysis of debris from the collision of the Cosmos 2251 and the Iridium 33 satellites. Science & Global Security 18, 87-118, 2010.

Figure captions

Figure 1. Spatial density of cataloged objects in low Earth orbit.
Figure 2. Gabbard diagram of the Fengyun 1C debris.
Figure 3. Gabbard diagram of the Cosmos 2251 and Iridium 33 debris.
Figure 4. Distribution of the Fengyun 1C, Cosmos 2251 and Iridium 33 cataloged debris in inclination vs. right ascension of the ascending node.
Figure 5. Snapshot of the Fengyun 1C, Cosmos 2251 and Iridium 33 cataloged debris geocentric right ascension and declination.
Figure 6. Distribution of the Fengyun 1C, Cosmos 2251 and Iridium 33 cataloged debris in inclination vs. argument of perigee.
Figure 7. Observed solar flux at 10.7 cm, in standard units of 10^{-22} Wm^{-2} Hz^{-1}, after the Fengyun 1C, Cosmos 2251 and Iridium 33 breakups.
Figure 8. Perigee altitude distribution of the three debris clouds at the reference epoch of the analysis.
Figure 9. Fengyun 1C debris: rescaled ballistic parameter distribution based on orbital decay analysis compared to the values obtained from B^*.
Figure 10. Cosmos 2251 debris: rescaled ballistic parameter distribution based on orbital decay analysis compared to the values obtained from B^*.
Figure 11. Iridium 33 debris: rescaled ballistic parameter distribution based on orbital decay analysis compared to the values obtained from B^*.
Figure 12. Area-to-mass ratio distributions of the Fengyun 1C, Cosmos 2251 and Iridium 33 debris clouds.
Figure 13. Time evolution, over the next 30 years, of the *A/M* distribution of the Fengyun 1C debris cloud.
Figure 14. Time evolution, over the next 30 years, of the *A/M* distribution of the Cosmos 2251 debris cloud.
Figure 15. Time evolution, over the next 30 years, of the *A/M* distribution of the Iridium 33 debris cloud.
Figure 16. Projected number of pieces of debris left in orbit, as a percentage of the cataloged objects on 20 April 2010, for the Fengyun 1C, Cosmos 2251 and Iridium 33 clouds.

Table 1

Situation in space at the reference epoch of the analysis (20 April 2010)
and perigee altitude distribution of the debris orbits

	Fengyun 1C	Cosmos 2251	Iridium 33
Cataloged Objects	2841	1228	512
Reentered Objects	85	50	22
Objects in Orbit	2756	1178	490
$P_H < 600$ km	516		
600 km $\leq P_H \leq$ 800 km	1144		
$P_H > 800$ km	1096		
$P_H < 500$ km		159	
500 km $\leq P_H \leq$ 700 km		466	
$P_H > 700$ km		553	
$P_H < 750$ km			209
$P_H \geq 750$ km			281

Table 2

Distribution of ballistic parameter scaling factors (defined as the ratio between the fitted values of B and those obtained from the average B^*) inferred from debris orbital decay analysis (mean value ± standard deviation)

	Fengyun 1C	**Cosmos 2251**	**Iridium 33**
$P_H < 600$ km	28.85 ± 16.05		
600 km $\leq P_H \leq$ 800 km	76.48 ± 21.33		
$P_H > 800$ km	73.09 ± 24.72		
$P_H < 500$ km		21.56 ± 8.12	
500 km $\leq P_H \leq$ 700 km		67.77 ± 12.34	
$P_H > 700$ km		80.05 ± 13.36	
$P_H < 750$ km			79.44 ± 10.95
$P_H \geq 750$ km			74.42 ± 13.65

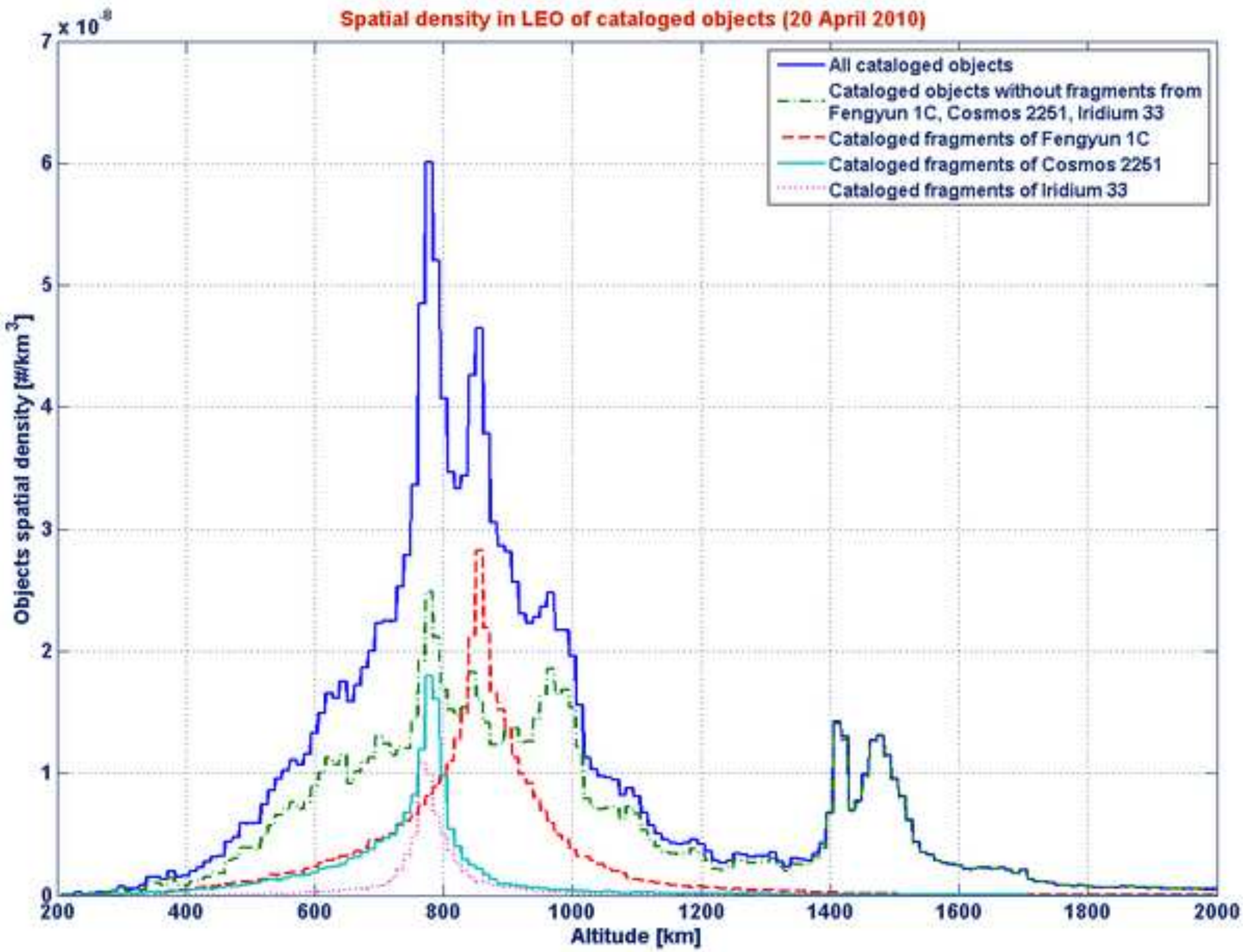

Spatial density in LEO of cataloged objects (20 April 2010)
x 10^-8
Objects spatial density [#/km^3]
Altitude [km]
All cataloged objects
Cataloged objects without fragments from Fengyun 1C, Cosmos 2251, Iridium 33
Cataloged fragments of Fengyun 1C
Cataloged fragments of Cosmos 2251
Cataloged fragments of Iridium 33
0
1
2
3
4
5
6
7
200
400
600
800
1000
1200
1400
1600
1800
2000

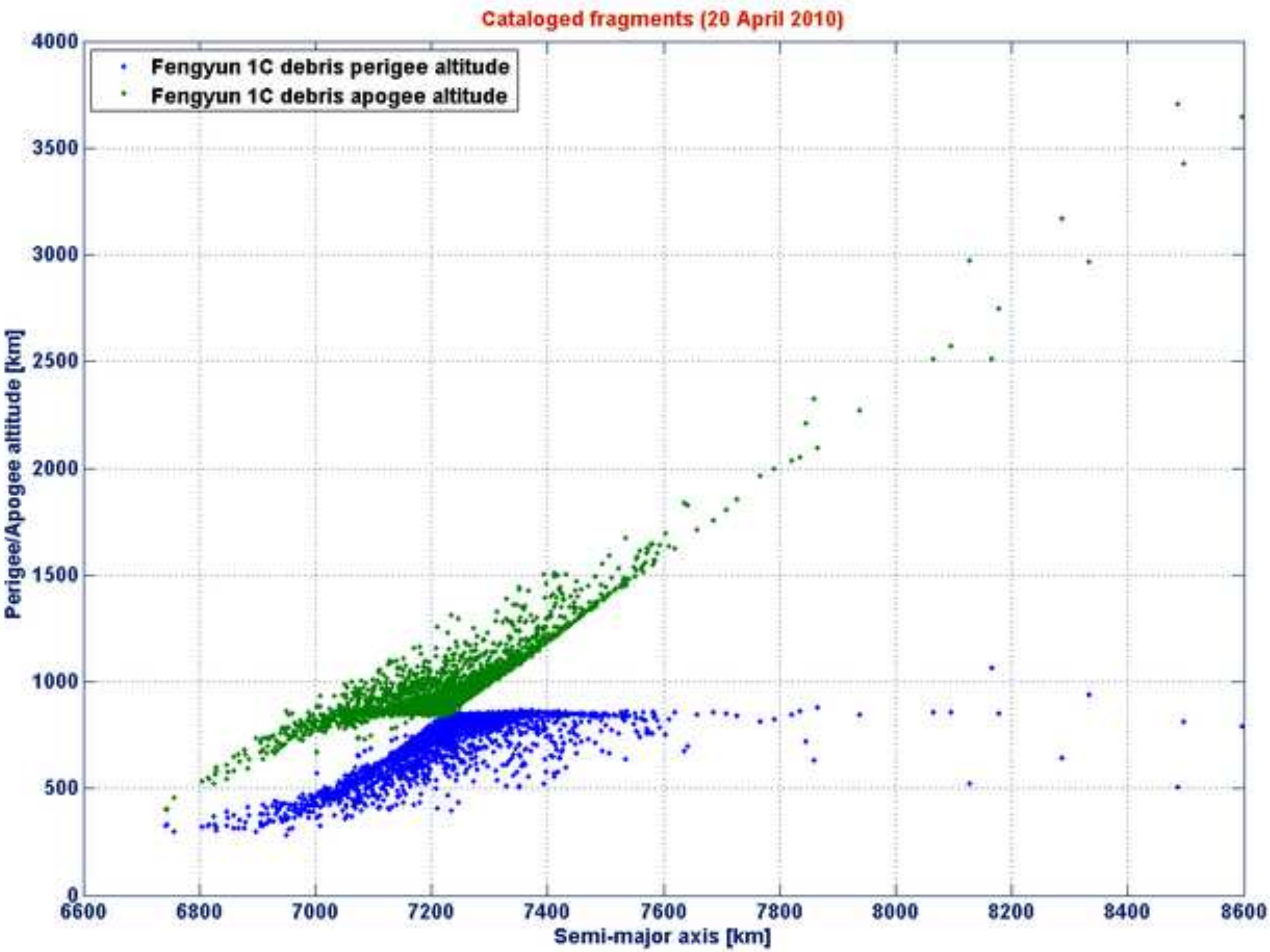
Cataloged fragments (20 April 2010)
Fengyun 1C debris perigee altitude
Fengyun 1C debris apogee altitude
Perigee/Apogee altitude [km]
Semi-major axis [km]
0
500
1000
1500
2000
2500
3000
3500
4000
6600
6800
7000
7200
7400
7600
7800
8000
8200
8400
8600

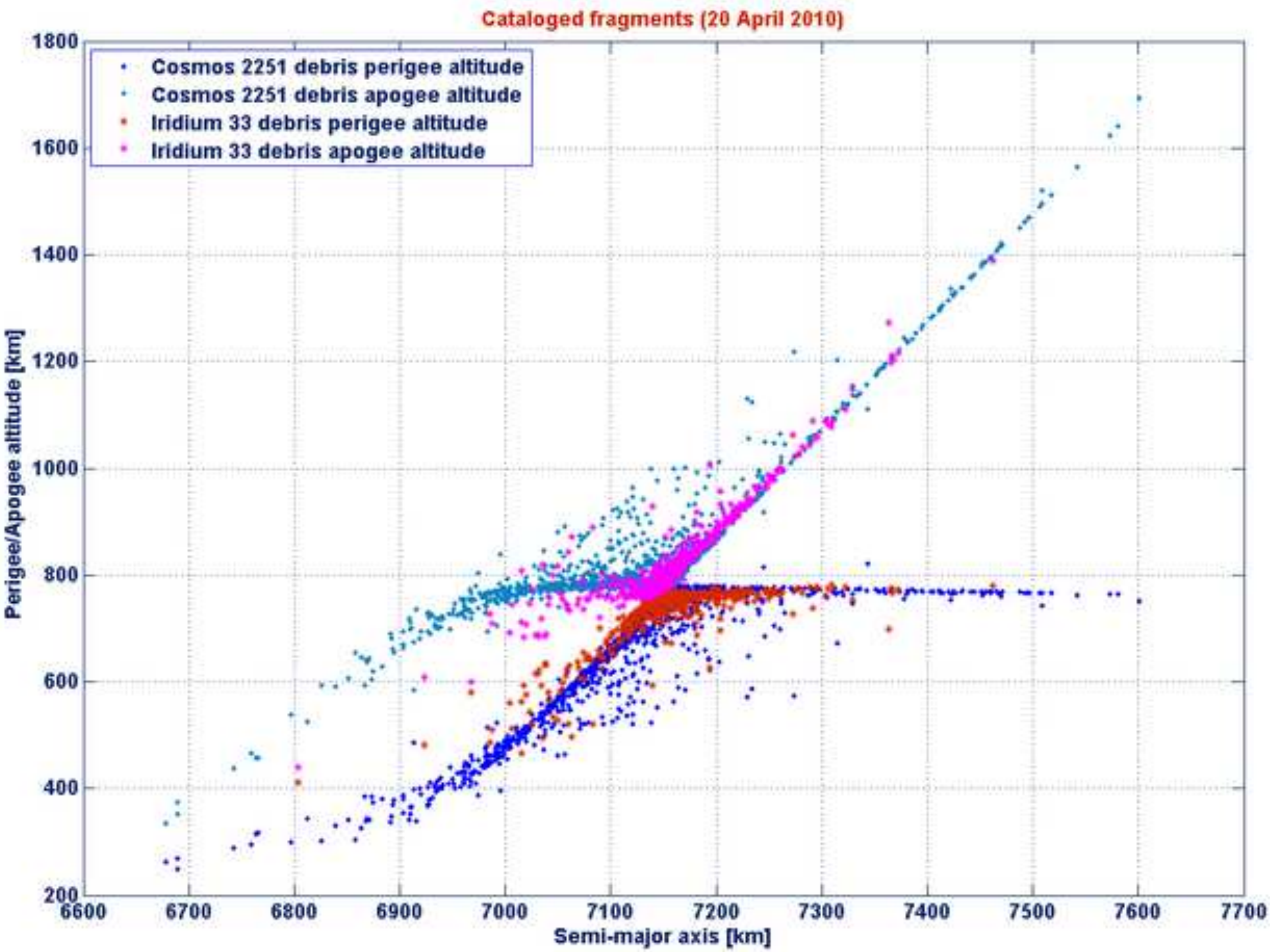

Cataloged fragments (20 April 2010)
Cosmos 2251 debris perigee altitude
Cosmos 2251 debris apogee altitude
Iridium 33 debris perigee altitude
Iridium 33 debris apogee altitude
Perigee/Apogee altitude [km]
Semi-major axis [km]
1800
1600
1400
1200
1000
800
600
400
200
6600
6700
6800
6900
7000
7100
7200
7300
7400
7500
7600
7700

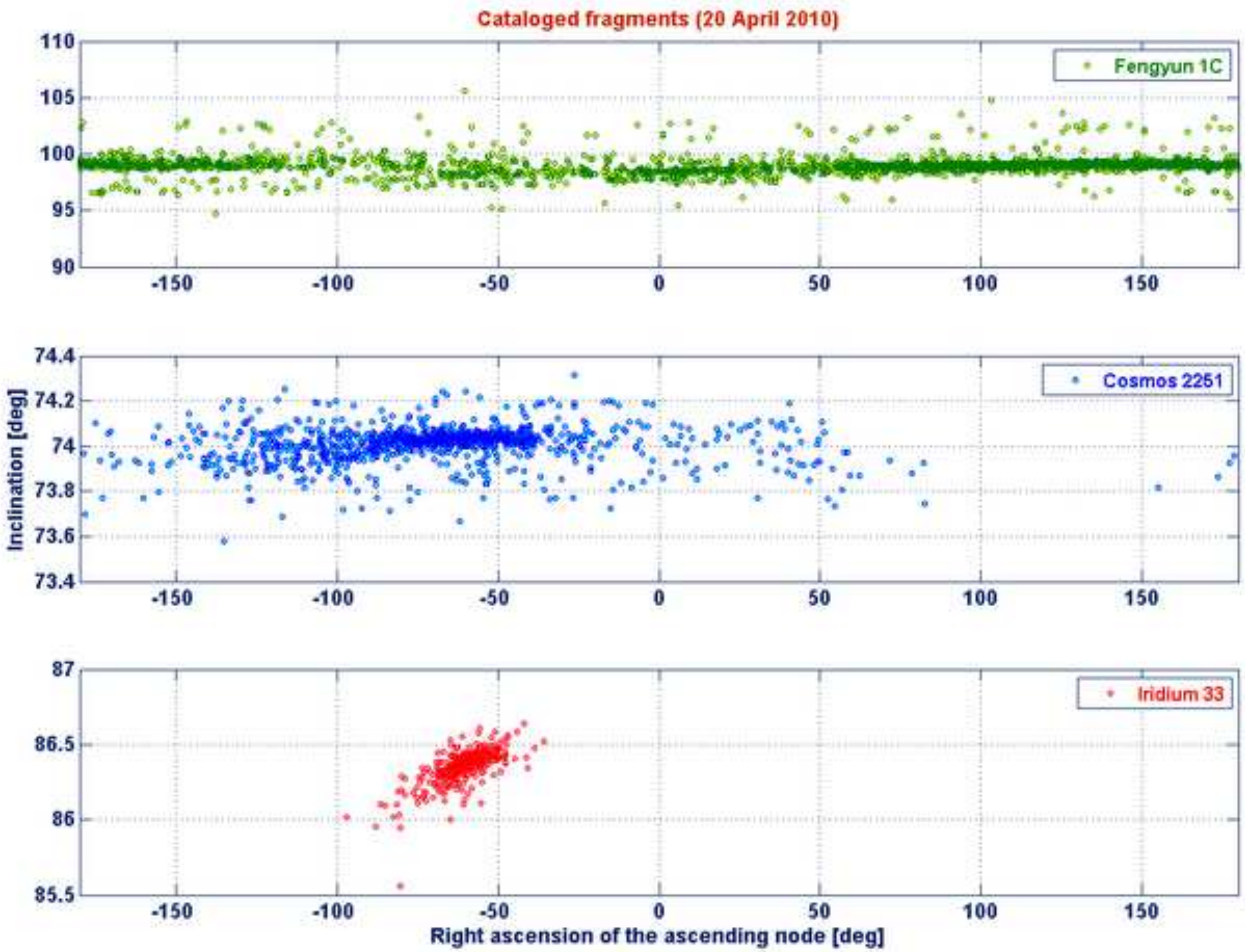

Cataloged fragments (20 April 2010)
Fengyun 1C
Cosmos 2251
Iridium 33
Inclination [deg]
Right ascension of the ascending node [deg]
110
105
100
95
90
74.4
74.2
74
73.8
73.6
73.4
87
86.5
86
85.5
-150
-100
-50
0
50
100
150

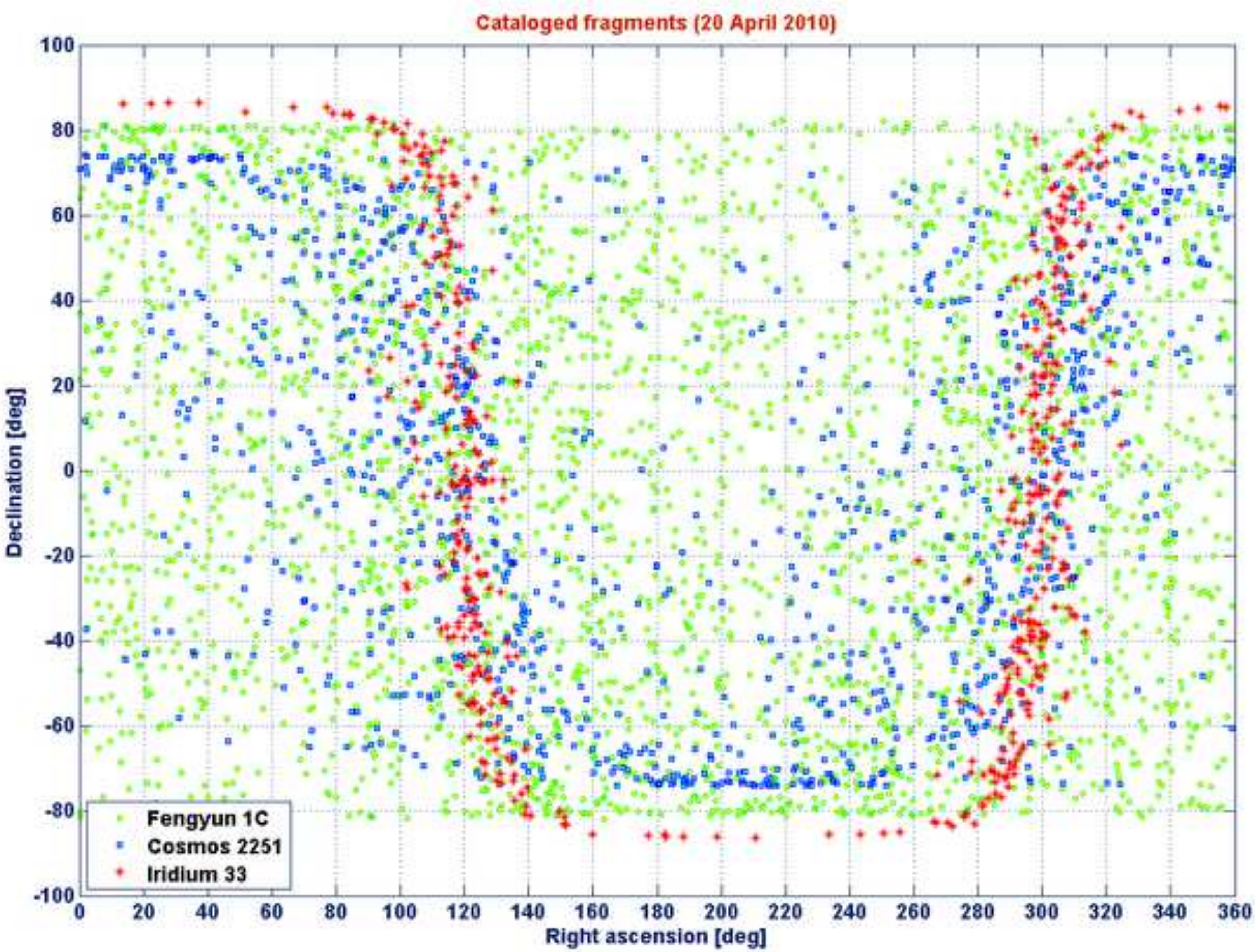
Cataloged fragments (20 April 2010)
Declination [deg]
Right ascension [deg]
100
80
60
40
20
0
-20
-40
-60
-80
-100
0
20
40
60
80
100
120
140
160
180
200
220
240
260
280
300
320
340
360
Fengyun 1C
Cosmos 2251
Iridium 33

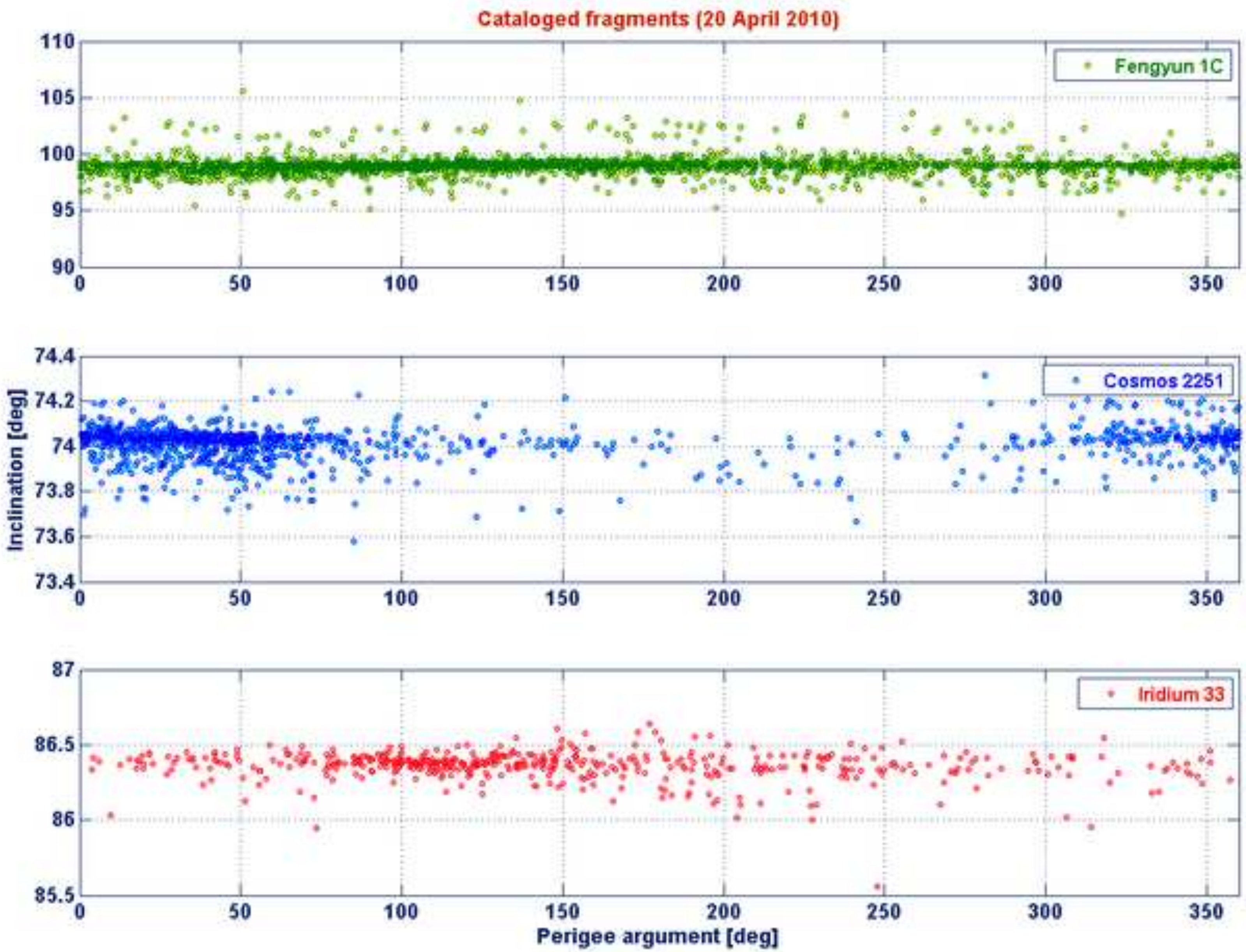
Cataloged fragments (20 April 2010)
Fengyun 1C
Cosmos 2251
Iridium 33
Inclination [deg]
Perigee argument [deg]
110
105
100
95
90
74.4
74.2
74
73.8
73.6
73.4
87
86.5
86
85.5
0
50
100
150
200
250
300
350

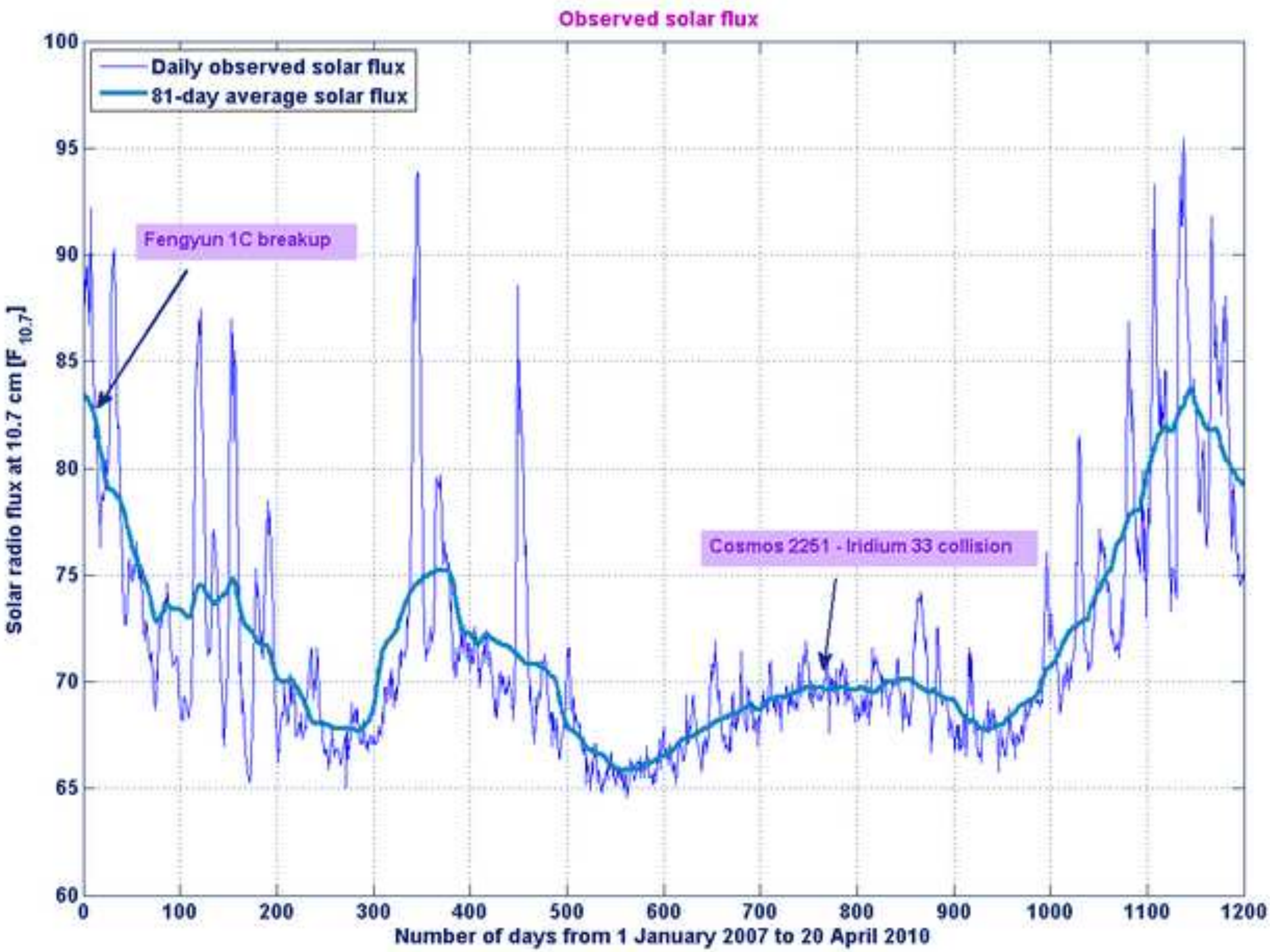
Observed solar flux
Daily observed solar flux
81-day average solar flux
Fengyun 1C breakup
Cosmos 2251 - Iridium 33 collision
Solar radio flux at 10.7 cm [$F_{10.7}$]
Number of days from 1 January 2007 to 20 April 2010
100
95
90
85
80
75
70
65
60
0
100
200
300
400
500
600
700
800
900
1000
1100
1200

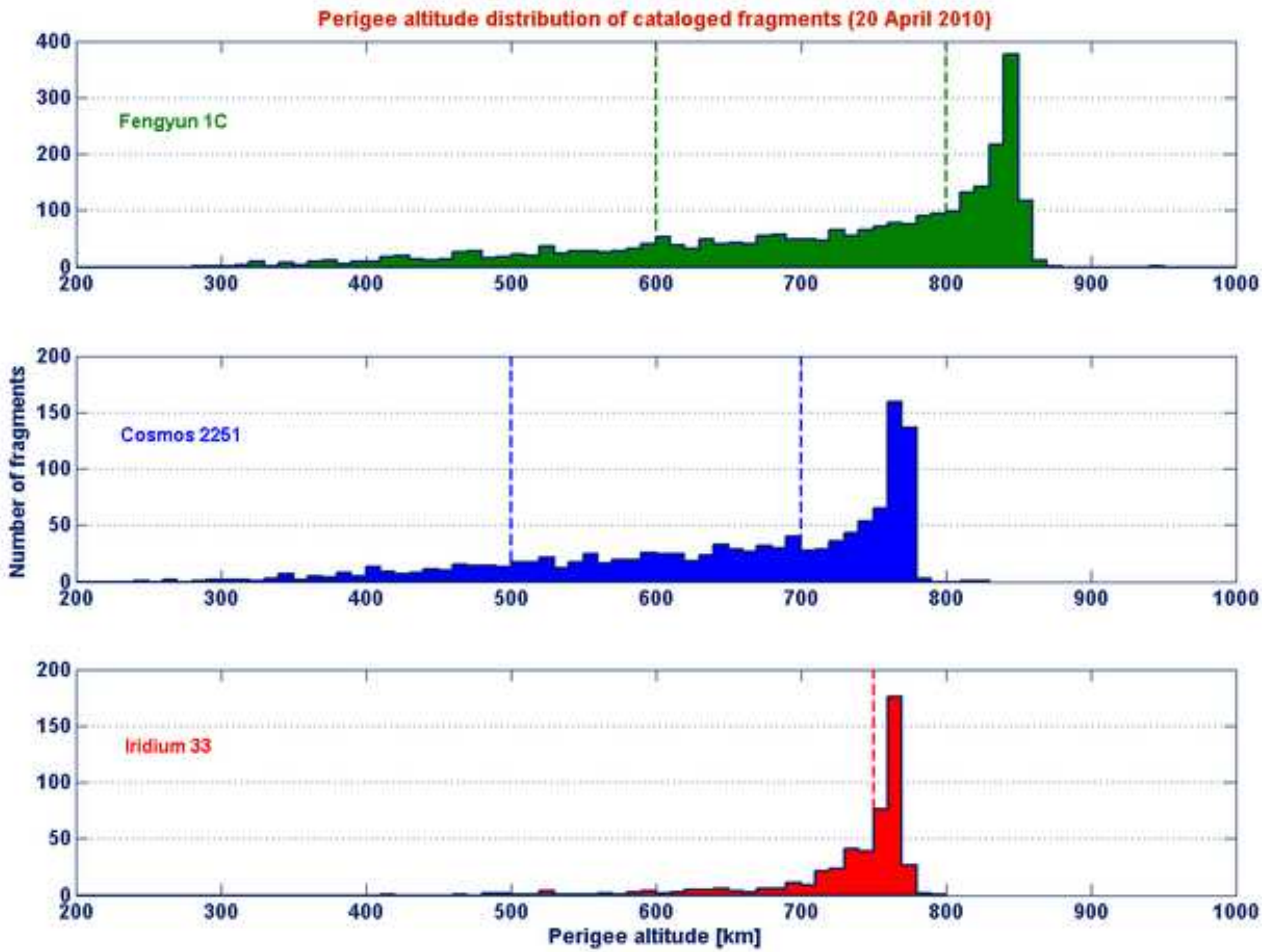

Perigee altitude distribution of cataloged fragments (20 April 2010)
Fengyun 1C
Cosmos 2251
Iridium 33
Number of fragments
Perigee altitude [km]
400
300
200
150
100
50
0
200
300
400
500
600
700
800
900
1000

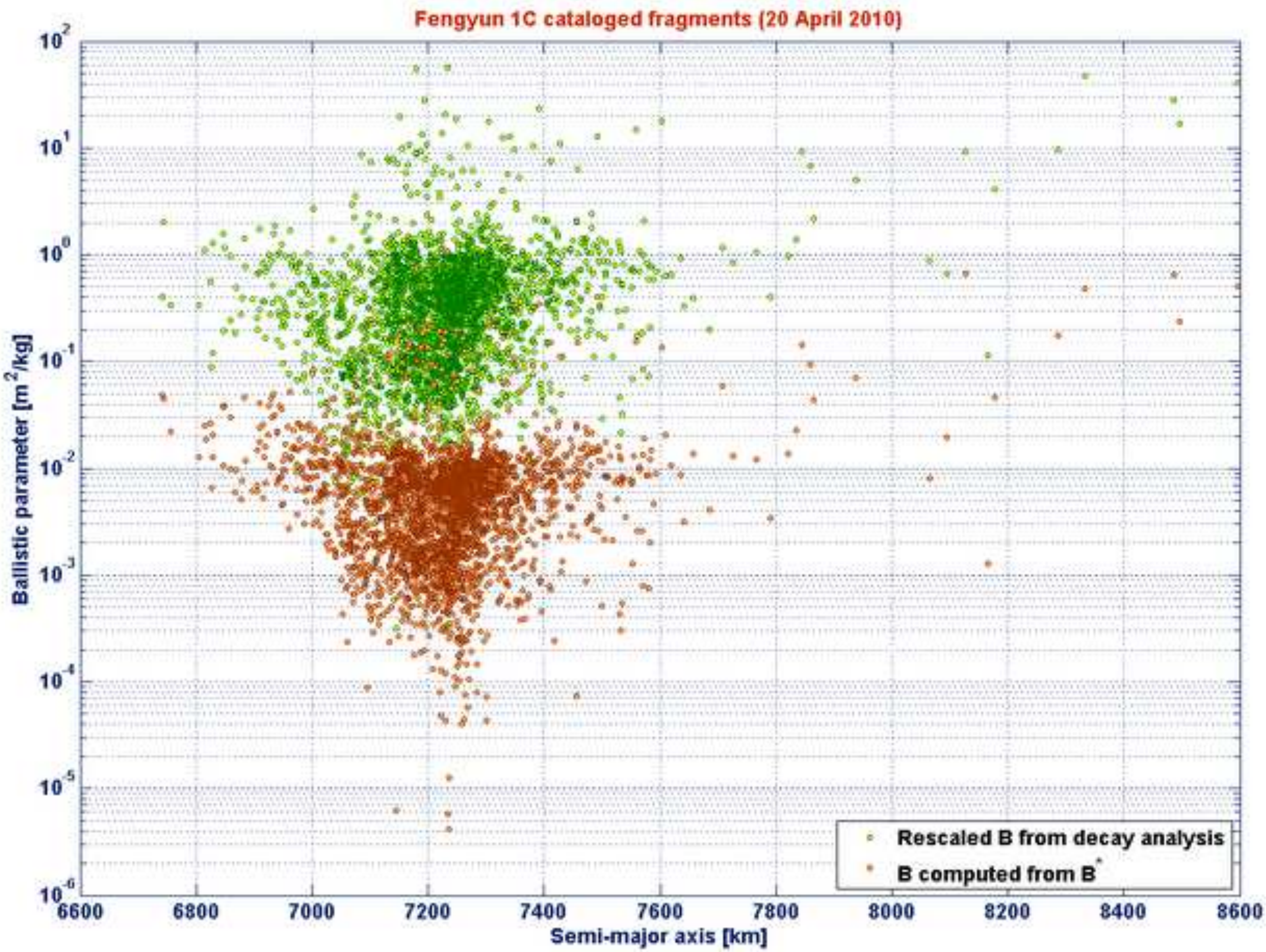
Fengyun 1C cataloged fragments (20 April 2010)
Ballistic parameter [m^2/kg]
Semi-major axis [km]
Rescaled B from decay analysis
B computed from B*
10^2
10^1
10^0
10^-1
10^-2
10^-3
10^-4
10^-5
10^-6
6600
6800
7000
7200
7400
7600
7800
8000
8200
8400
8600

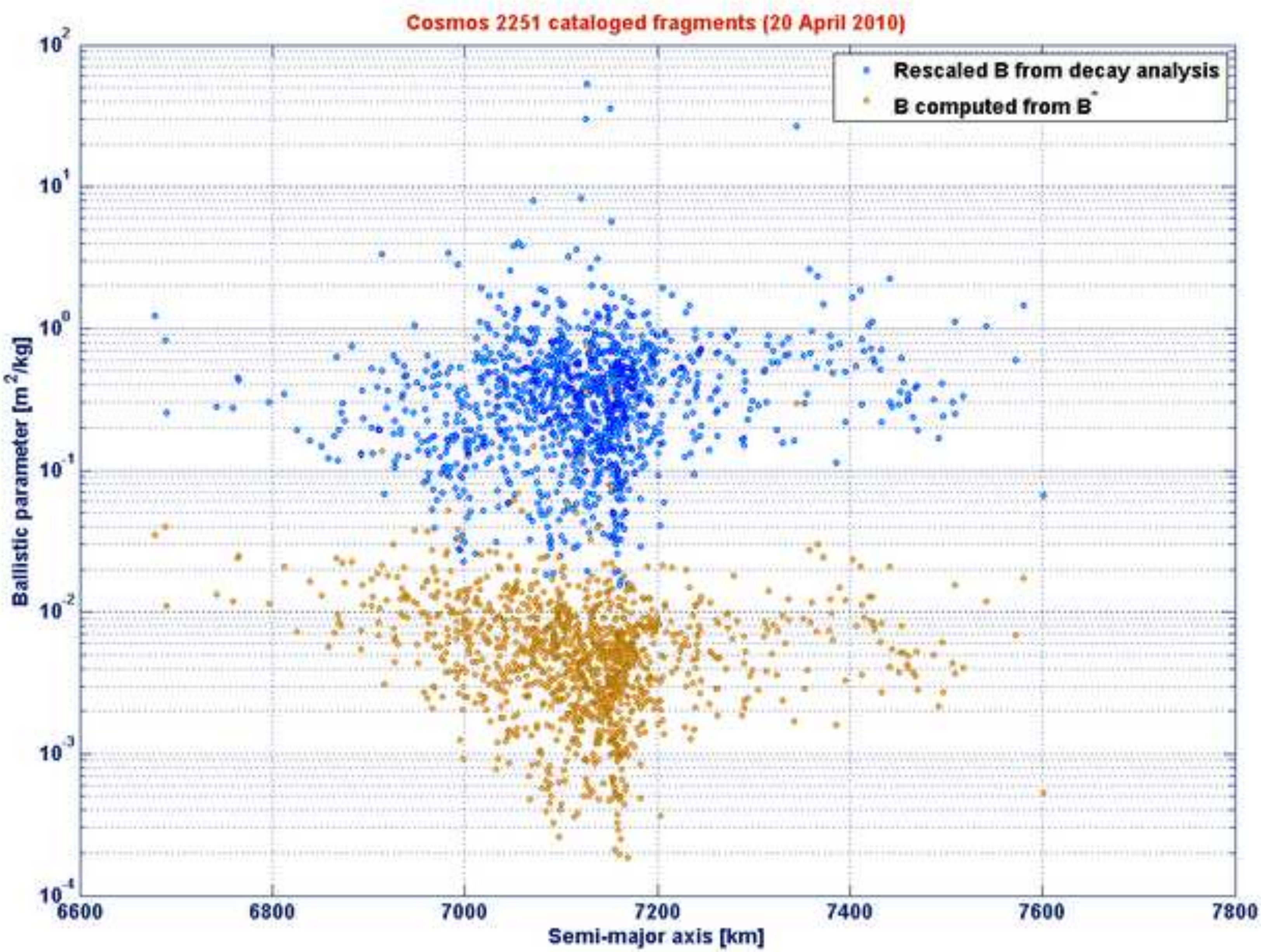

Cosmos 2251 cataloged fragments (20 April 2010)
Rescaled B from decay analysis
B computed from B*
Ballistic parameter [m 2/kg]
Semi-major axis [km]
10^2
10^1
10^0
10^-1
10^-2
10^-3
10^-4
6600
6800
7000
7200
7400
7600
7800

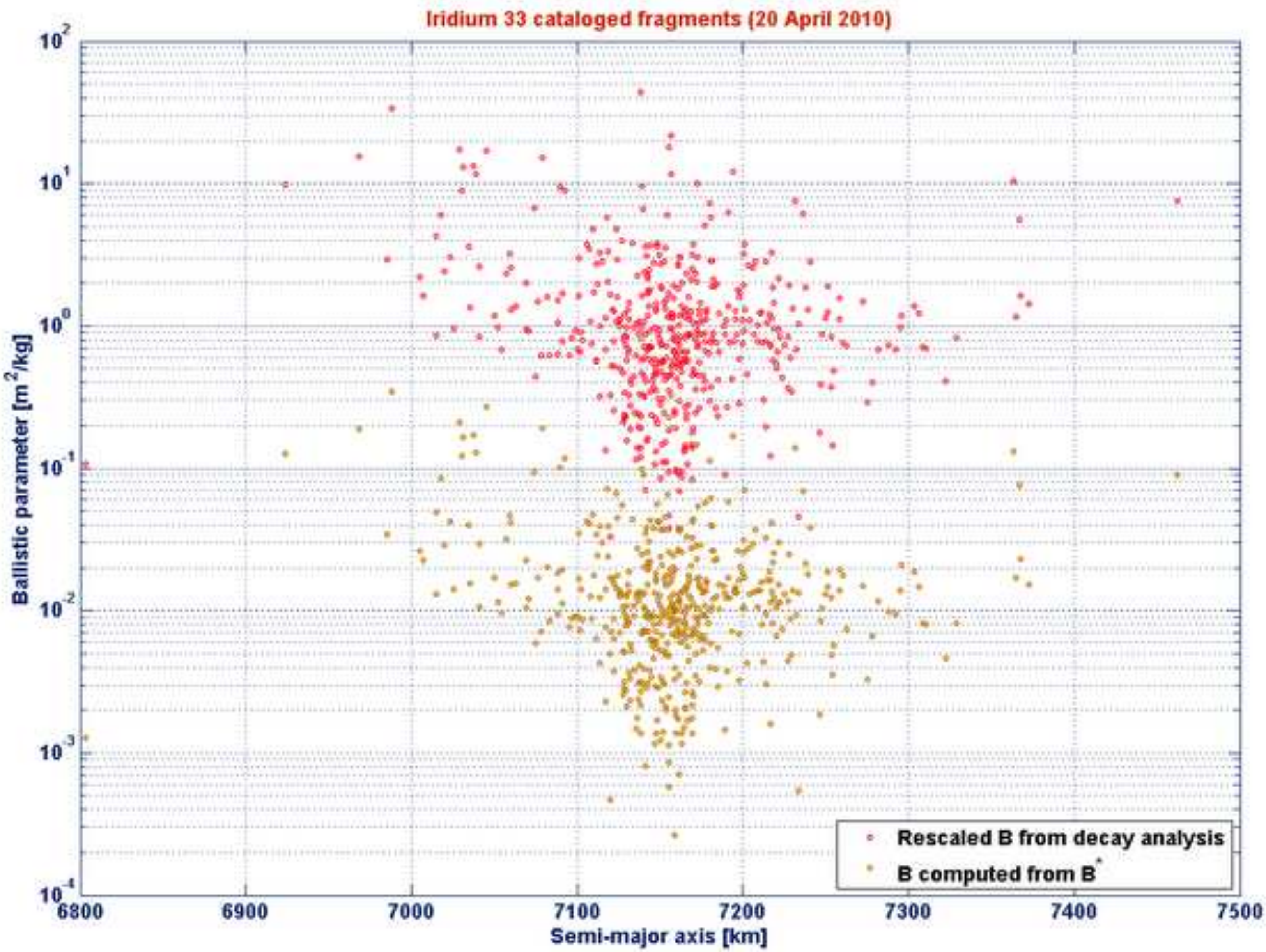

Iridium 33 cataloged fragments (20 April 2010)
Ballistic parameter [m 2/kg]
Semi-major axis [km]
Rescaled B from decay analysis
B computed from B*
10^2
10^1
10^0
10^-1
10^-2
10^-3
10^-4
6800
6900
7000
7100
7200
7300
7400
7500

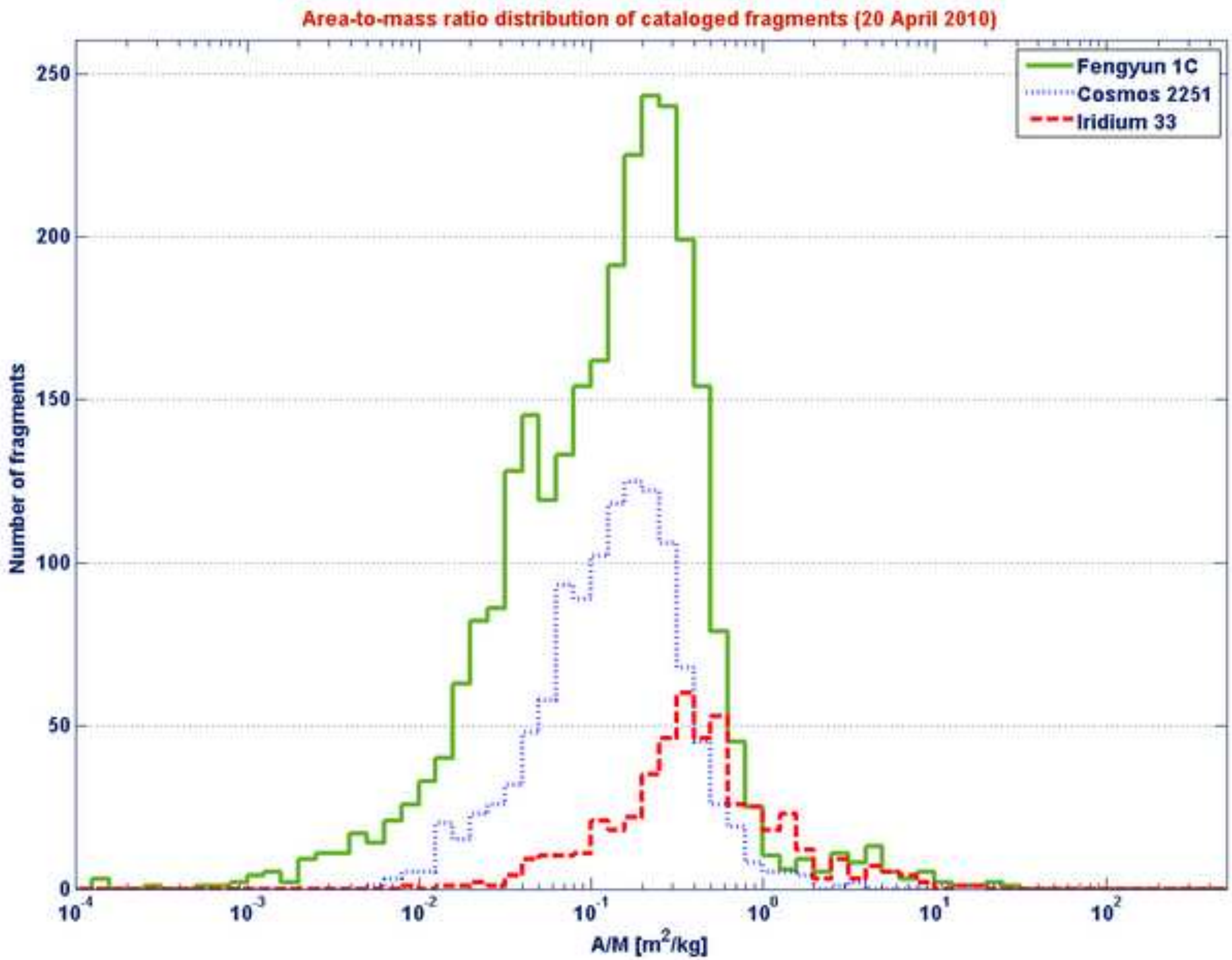

Area-to-mass ratio distribution of cataloged fragments (20 April 2010)
Fengyun 1C
Cosmos 2251
Iridium 33
Number of fragments
250
200
150
100
50
0
10^{-4}
10^{-3}
10^{-2}
10^{-1}
10^{0}
10^{1}
10^{2}
A/M [m^2/kg]

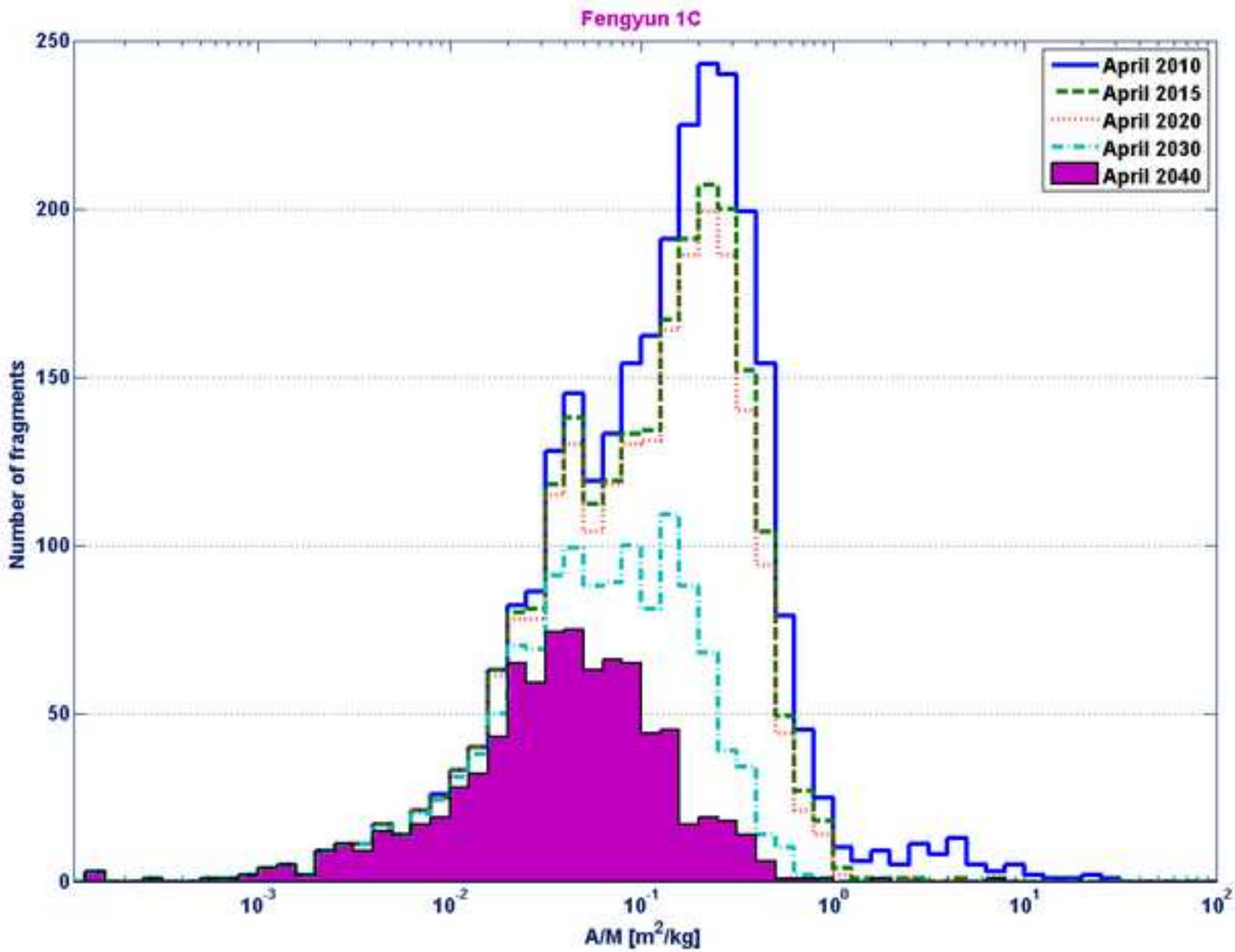
Fengyun 1C
Number of fragments
A/M [m^2/kg]
April 2010
April 2015
April 2020
April 2030
April 2040
0
50
100
150
200
250
10^{-3}
10^{-2}
10^{-1}
10^{0}
10^{1}
10^{2}

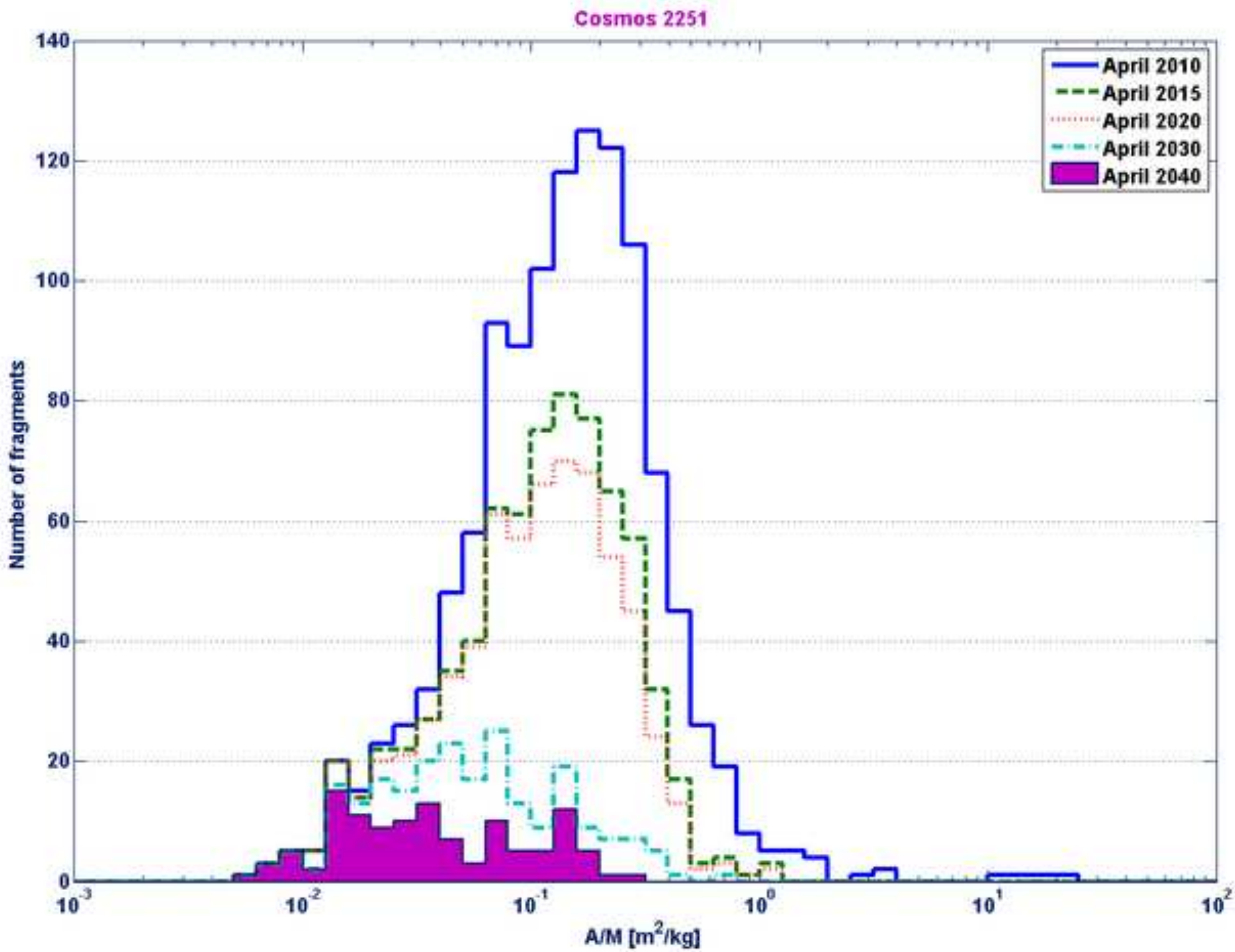
Cosmos 2251
Number of fragments
A/M [m^2/kg]
April 2010
April 2015
April 2020
April 2030
April 2040
140
120
100
80
60
40
20
0
10^{-3}
10^{-2}
10^{-1}
10^{0}
10^{1}
10^{2}

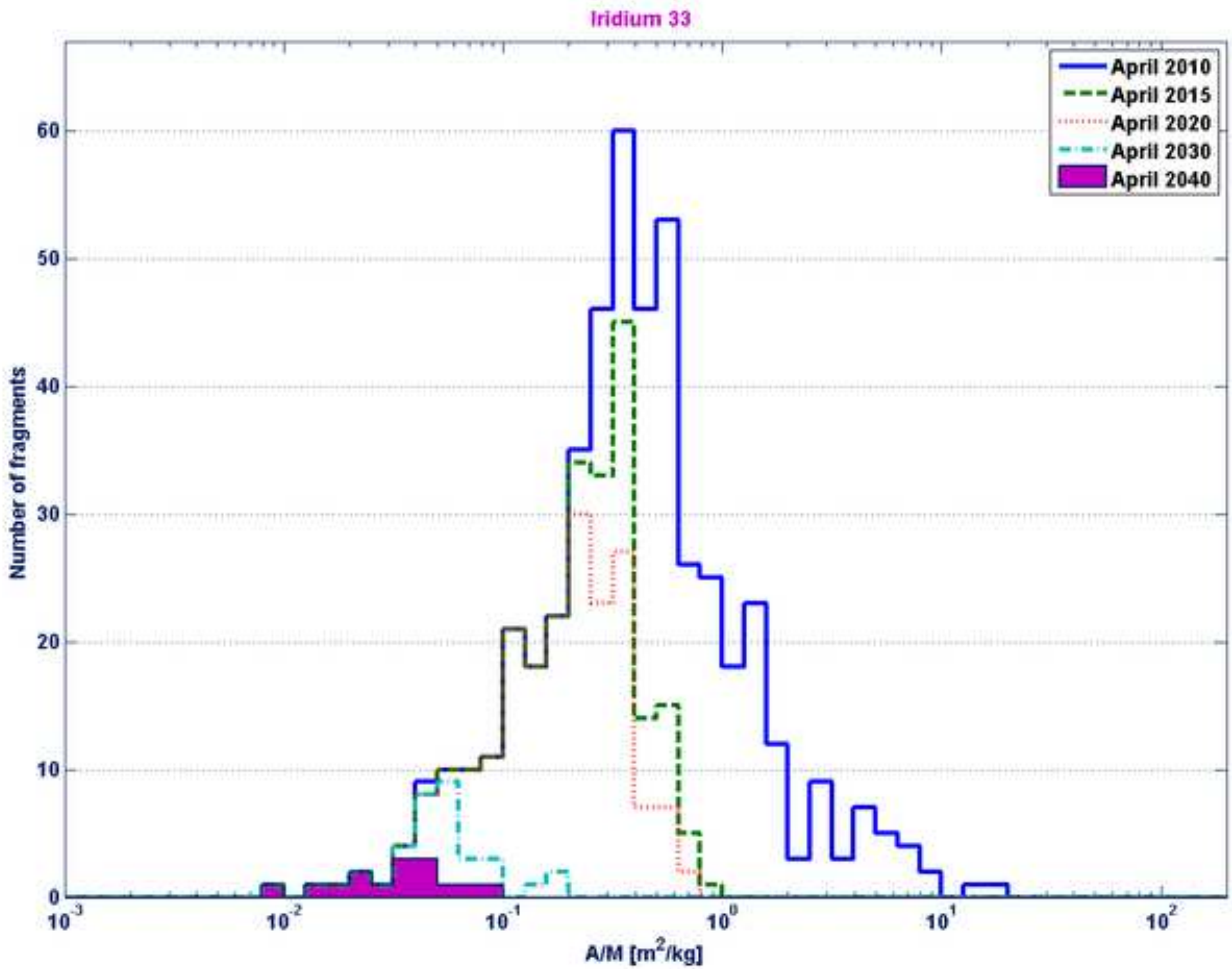

Iridium 33
April 2010
April 2015
April 2020
April 2030
April 2040
Number of fragments
0
10
20
30
40
50
60
10^{-3}
10^{-2}
10^{-1}
10^{0}
10^{1}
10^{2}
A/M [m^2/kg]

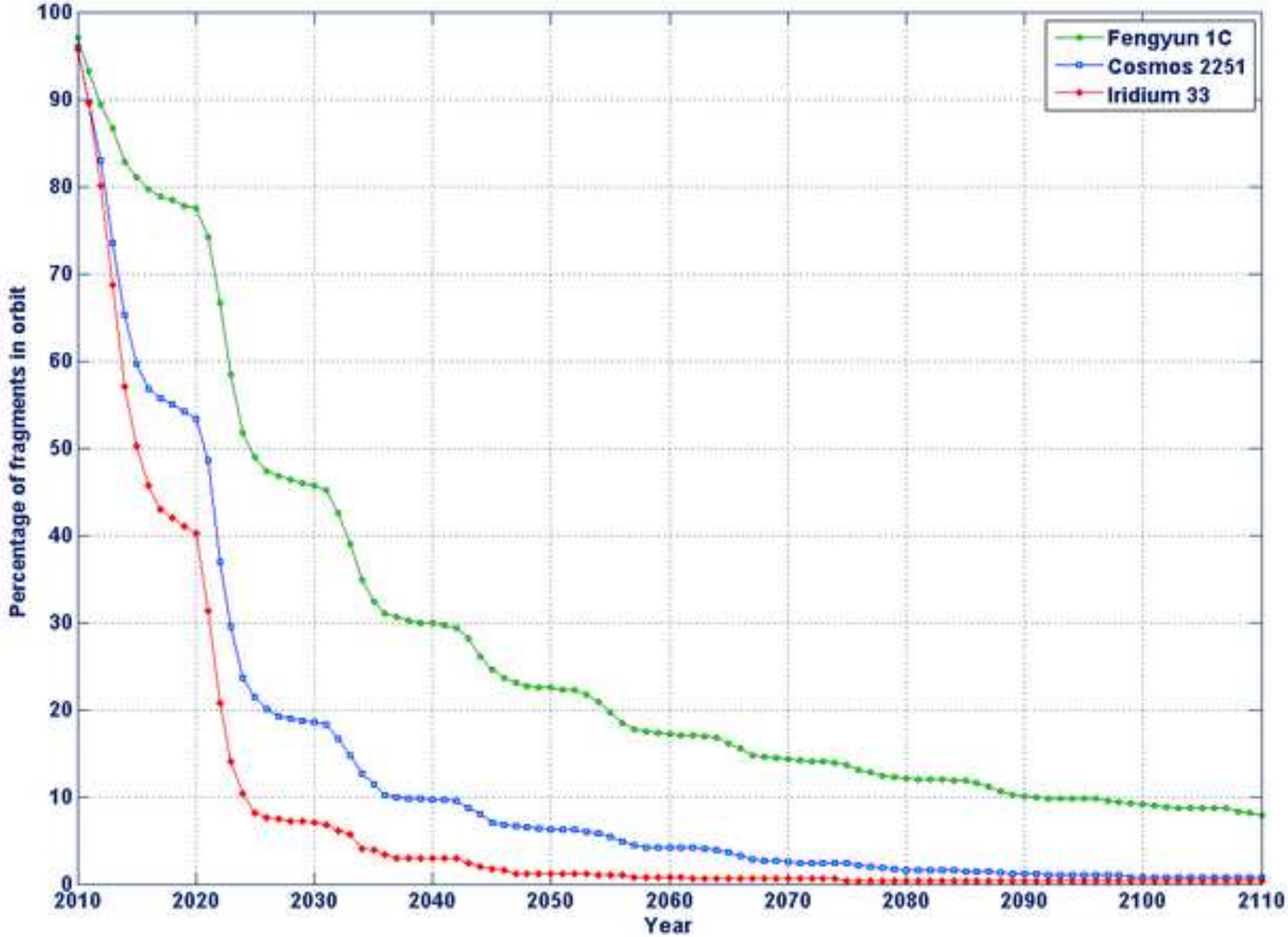
Fengyun 1C
Cosmos 2251
Iridium 33
Percentage of fragments in orbit
Year
0
10
20
30
40
50
60
70
80
90
100
2010
2020
2030
2040
2050
2060
2070
2080
2090
2100
2110

Keywords: On-orbit collision; Fengyun 1C; Cosmos 2251; Iridium 33; Debris cloud evolution; Ballistic parameter.